Construction of High Performance Balanced Symmetric Multifilter Banks and Application in Image Processing

Zhaohui Zeng
College of Information and Engineering of Xiangtan University, Xiangtan, China
Email:zzh@xtu.edu.cn

Yajun Liu*
Business school of Xiangtan University, Xiangtan, China
Email: lyj@xtu.edu.cn

***Abstract*—Multifilter banks having all properties of symmetry, balancing, optimum time-frequency resolution, arbitrary order vanishing moment, orthogonality and compactly supported together are constructed for the first time. Thus overcome the shortcoming of the present orthogonal optimum time-frequency resolution multifilter banks that have only the properties of symmetry and 2-order vanishing moment but not balanced. Balanced symmetric orthogonal multifilter banks with good regularity and time-frequency resolution are also provided. Due to the excellent properties, application experiments in image denoising and compression showed that, most of our multifilter banks outperform the best tools known as multiwavelet SA4 and wavelet CDF9-7 in denoising with texture image and smooth image. They also outperform multiwavelet SA4 or approximate wavelet DB4 in compression with texture image.**

***Index Terms*—multifilter bank, symmetry, balanced, vanishing moment, time-frequency resolution, regularity**

I. INTRODUCTION

Multiwavelet is attracting more and more attention for its good properties such as orthogonality, symmetry, compactly supported, high vanishing moment and balance contrast with the traditional wavelet. These properties, along with optimum time-frequency resolution (OPTFR) are all very important in image processing. Generally, multiwavelet with i) orthogonality can keep energy conserved and make less redundancy; ii) the property of symmetry adapts to the function of human eyes. Image distortion can be reduced by symmetric extension transform of signals with finite length; iii) higher vanishing moment can lead to energy concentration in the part of low-frequency, with more zero values in the high frequency part; iv) in image processing, smooth error is more tolerable for human eyes than non-regular error that has the same energy, which emphasizes the importance of regularity for multiwavelet to improve the quality of reconstructed image; v) the property of locational time-frequency also plays a vital role in the great task of coding with stable image compacting or digital video[1][2], especially when extracting high frequency components such as textures, edges and movements; vi) in image denoising with balanced multiwavelet, the aliasing of low-frequency and high-frequency signals can be avoid, and good performance can be expected without pre-filtering. Therefore, how to design the balanced multifilter banks with all the properties of symmetry, time-frequency resolution, high vanishing moment, regularity and orthogonality together is a valuable issue to pay attention to.

In 1998, Jiang[4] first introduced the concept of time-frequency resolution of multiwavelets. Using OPTFR orthogonal multiwavelets, Jiang got some ideal result in image compressing. To present, Jiang's work is known as the best in dealing with OPTFR multiwavelet and its application. However, with only 2-order vanishing moment, the capability of approximating to smooth function for Jiang's OPTFR orthogonal multiwavelets is limited. Moreover, the orthogonal OPTFR multiwavelets in Jiang[4] are not balanced. Although we can get balanced orthogonal scaling functions and mutliwavelets by rotating them for $\pi/4$ angle, the symmetry of the scaling functions, multiwavelets and their multifilter banks would be lost, which are not optimum in its time-frequency property any longer. Later in 2000, Jiang[6] introduced the parameterized representation of the symmetric orthogonal multiwavelet with different length of filter banks. But he only provided the example of the smoothest multifilter banks, without considering the time-frequency property.

With the properties of symmetry, balancing, optimum time-frequency resolution, arbitrary order vanishing moment and orthogonality synthetically concerned, construction method of multiwavelets is improved, and balanced symmetric orthogonal multifilter banks with arbitrary vanishing moment and optimum in time-frequency resolution were obtained. Furthermore, application in image denoising and compression showed their advantages.

II. RELEVANT THEORY

Suppose a set of compactly supported scaling functions $\phi_1,\cdots,\phi_r \in L^2(R)$ whose integer translates form an

* Corresponding author. Tel: 86-731-58293939. Supported by a grant from Hunan Education Bureau(09C963).

doi:10.4304/jcp.5.7.1038-1045

orthogonal basis of V_0, then (V_j) is called an orthogonal MRA. If the integer translates of a set functions $\psi_1,\cdots,\psi_r$ form an orthogonal basis of W_0, then $\psi_1,\cdots,\psi_r$ is a set of orthogonal multiwavelets. Assume that P, Q are $r\times r$ matrix filter with matrix coefficient P_k and Q_k satisfying $P_k=0_r$ and $Q_k=0_r$ ($k<0$ and $k>N$, $N\in Z_+$), and $\Phi=(\phi_1,\cdots,\phi_r)^T$, $\Psi=(\psi_1,\cdots,\psi_r)^T$ are compactly supported refinable vector-valued function satisfying

$$\Phi(x)=2\sum_{k=0}^{N}P_k\Phi(2x-k)\ ,\ \Psi(x)=2\sum_{k=0}^{N}Q_k\Phi(2x-k) \qquad (1)$$

or equivalently satisfying

$$\hat\Phi(\omega)=P(\omega/2)\hat\Phi(\omega/2)\ ,\ \hat\Psi(\omega)=P(\omega/2)\hat\Psi(\omega/2)\ , \qquad (2)$$

where $P(\omega)=\sum_{k=0}^{N}P_ke^{-ik\omega}$, $Q(\omega)=\sum_{k=0}^{N}Q_ke^{-ik\omega}$. If Ψ is a compactly supported orthogonal multiwavelet, then P, Q generate an orthogonal multiwavelet basis. The pair $\{P,Q\}$ is called multifilter bank, and P (Q, respectively) is called a matrix lowpass filter (matrix highpass filter, respectively). For a multifilter bank, the matrix filters P, Q are called finite impulse responses (FIR).

If the compactly supported refinable vector Φ is stable, then $\hat\Phi(\omega)=\lim_{n\to\infty}\hat\Phi_n(\omega)$, where

$$\hat\Phi_n(\omega):=\hat\Upsilon_n(\omega)v_0\frac{\sin\left(\omega/2^{n+1}\right)}{\omega/2^{n+1}}e^{-i\omega/2^{n+1}} \qquad (3)$$

$$\hat\Upsilon_n(\omega):=P\left(\frac{\omega}{2}\right)\cdots P\left(\frac{\omega}{2^n}\right),$$

and v_0 is the normalized right 1-eigenvector of $P(0)$ [7] [8].

If Ψ_n approximate Ψ, then

$$\hat\Psi_n(\omega)=Q(\omega/2)\hat\Phi_n(\omega/2)\ . \qquad (4)$$

Let $H_m(\omega)$ denote the modulation matrix of an FIR multifilter bank $\{P,Q\}$ defined by

$$H_m(\omega):=\begin{bmatrix}P(\omega) & P(\omega+\pi)\\ Q(\omega) & Q(\omega+\pi)\end{bmatrix}.$$

If $\{P,Q\}$ generates an orthogonal multiwavelet, then $H_m(\omega)$ is lossless, i.e., $H_m(\omega)$ is unitary for all ω:

$$P(\omega)P^*(\omega)+P(\omega+\pi)P^*(\omega+\pi)=I_r,\omega\in[-\pi,\pi],$$
$$Q(\omega)Q^*(\omega)+Q(\omega+\pi)Q^*(\omega+\pi)=I_r,\omega\in[-\pi,\pi],$$
$$P(\omega)Q^*(\omega)+P(\omega+\pi)Q^*(\omega+\pi)=0_r,\omega\in[-\pi,\pi],$$

where B^* denotes the Hermitian adjoint of the matrix B, I_r and 0_r denote the $r\times r$ identity matrix and zero matrix respectively[13].

Let H_N denote the space of all $r\times r$ matrices with trigonometric polynomial entries whose Fourier coefficients are real and supported in $[1-N,N-1]$. The transition operator T_P corresponding to P is defined on H_N by

$$\mathrm{T}_PH(\omega):=P(\frac{\omega}{2})H(\frac{\omega}{2})P^*(\frac{\omega}{2})+P(\frac{\omega}{2}+\pi)H(\frac{\omega}{2}+\pi)P^*(\frac{\omega}{2}+\pi),H\in\mathrm{H}_N$$

Thus, the representation matrix T_P of the operator T_P is

$$T_P:=(2A_{2i-j})_{1-N\le i,j\le N-1}\ ,$$

where $A_j:=\sum_{k=0}^{N}P_{k-j}\otimes P_k$.

If a matrix or an operator A satisfier Condition E, then the spectral radius of A is 1, 1 is the unique eigenvalue of A on the unit circle and 1 is simple.

If transition operator T_P associated with P satisfies Condition E, then there exists a unique compactly supported solution Φ with $\hat\Phi(0)\ne0$. Furthermore Φ is a scaling function, i.e. Φ generates a multiwavelet Ψ [3]. In this case, $\{P,Q\}$ generates the scaling function Φ and the multiwavelet Ψ.

For $s\ge0$, it is said that a function f is in Sobolev space $W^s(R)$ if $(1+|\omega|^2)^{s/2}\hat\Phi(\omega)\in L^2(R)$, where $\hat f$ denotes the Fourier transform of f.

If the compactly supported refinable vector Φ is stable, then the property that Φ has approximation of order m is equivalent to that P satisfies the vanishing moment conditions of order m [10].

Proposition 1: It is said that P satisfies the vanishing moment conditions of order m if there exist real $1\times r$ row vectors with $l_0^0\ne0$, $0\le\beta<m$, such that

$$\begin{cases}\sum_{0\le\alpha\le\beta}\binom{\beta}{\alpha}(2i)^{\alpha-\beta}l_0^\alpha D^{\beta-\alpha}P(0)=2^{-\beta}l_0^\beta,\\ \sum_{0\le\alpha\le\beta}\binom{\beta}{\alpha}(2i)^{\alpha-\beta}l_0^\alpha D^{\beta-\alpha}P(\pi)=0,\end{cases}$$

where $D^{\beta-\alpha}P(\omega)$ denotes the matrix formed by the ($\beta-\alpha$)th derivatives of the entries of $P(\omega)$ [10].

Lemma 1: If P satisfies the vanishing moment conditions of order 1, then

$$l_0^0P(0)=l_0^0,l_0^0P(\pi)=0\ , \qquad (5)$$

where the real $1\times r$ row vector $l_0^0\ne0$.

Difinition 1. An orthonormal multiwavelet system is said to be balanced (of order 1) if and only if the lowpass synthesis operator L^T preserves the constant signals, i.e., $L^Tu_0=u_0$, $u_0=(\cdots,1,1,1,1,\cdots)^T$.

Symmetric properties of multifilter banks are very important in image applications. For symmetric filters, symmetric extension transforms of the finite length signals can be carried out, which will improve the rate-distortion performance in image compression. This paper only discuss symmetric filters with the coefficients h_j, g_j having the form

$$[h_0,h_1,\cdots,h_{2\gamma-1},h_{2\gamma},h_{2\gamma+1}]=$$
$$\left[\begin{bmatrix}a_0&a_1\\b_0&b_1\end{bmatrix},\begin{bmatrix}a_2&a_3\\b_2&b_3\end{bmatrix},\cdots,\begin{bmatrix}a_1&a_0\\b_5&b_4\end{bmatrix},\begin{bmatrix}0&0\\b_3&b_2\end{bmatrix}\begin{bmatrix}0&0\\b_1&b_0\end{bmatrix}\right],$$

$$[g_0, g_1, \cdots, g_{2\gamma-1}, g_{2\gamma}, g_{2\gamma+1}] =$$
$$\left[\begin{bmatrix} c_0 & c_1 \\ d_0 & d_1 \end{bmatrix}, \begin{bmatrix} c_2 & c_3 \\ d_2 & d_3 \end{bmatrix}, \cdots, \begin{bmatrix} -c_1 & -c_0 \\ -d_5 & -d_4 \end{bmatrix}, \begin{bmatrix} 0 & 0 \\ -d_3 & -d_2 \end{bmatrix}, \begin{bmatrix} 0 & 0 \\ -d_1 & -d_0 \end{bmatrix}\right], \quad (6)$$

for some $a_j, b_j, c_j, d_j \in R$, $h_j, g_j = 0$, $j < 0$, $j > 2\gamma + 1$. The corresponding scaling functions Φ and multiwavelets Ψ are not symmetric or antisymmetric. However, as multifilter banks, the rows of $[h_0, h_1, \cdots, h_{2\gamma-1}, h_{2\gamma}, h_{2\gamma+1}]$ and $[g_0, g_1, \cdots, g_{2\gamma-1}, g_{2\gamma}, g_{2\gamma+1}]$ are symmetric and antisymmetric respectively, which are more important than the symmetry of Φ, Ψ in image applications.

In this paper, we will discuss orthogonal multifilter banks $\{{}_\gamma P, {}_\gamma Q\}$ with ${}_\gamma P$, ${}_\gamma Q$ having the form of (6). It is obtained that (6) is equivalent to

$$z^{-(2\gamma+1)} \begin{bmatrix} z^2 & 0 \\ 0 & 1 \end{bmatrix} {}_\gamma P(-\omega) J_2 = {}_\gamma P(\omega),$$
$$z^{-(2\gamma+1)} \begin{bmatrix} -z^{2l} & 0 \\ 0 & -1 \end{bmatrix} {}_\gamma Q(-\omega) J_2 = {}_\gamma Q(\omega), \quad (7)$$

for some integer l and that $s_1 = \pm 1$, $s_2 = \pm 1$.

Lemma 2. Assume that the multfilter bank $\{{}_\gamma P, {}_\gamma Q\}$ is orthogonal and that ${}_\gamma P$, ${}_\gamma Q$ satisfy (7), then $s_1 = s_2 = -1$.

Proposition 2. A Causal FIR filter bank $\{{}_\gamma P, {}_\gamma Q\}$ is orthogonal and satisfies (7) if and only if it can be factorized as

$$\begin{bmatrix} {}_\gamma P(\omega) \\ {}_\gamma Q(\omega) \end{bmatrix} = \frac{\sqrt{2}}{4}(I_4 - B_0 + B_0 z^{-2}) \times$$
$$U_{\gamma-1}(z^2) \cdots U_1(z^2) \begin{bmatrix} w_0 & w_0 D_0 \\ v_0 & -v_0 D_0 \end{bmatrix} \begin{bmatrix} I_2 & \\ z^{-1} I_2 & \end{bmatrix} \begin{bmatrix} 1 & 1 \\ -1 & 1 \end{bmatrix}, \quad (8)$$

where $w_0, v_0 \in O(2)$, and $B_0 := \begin{bmatrix} 0 & 0 \\ 0 & b_0 \end{bmatrix}$,

$b_0 := \frac{1}{2}(1, 0, \pm 1)^T (1, 0, \pm 1)$,

$U_k(z) = \frac{1}{2}\begin{bmatrix} I_2 & u_k \\ u_k^T & I_2 \end{bmatrix} + \frac{1}{2}\begin{bmatrix} I_2 & -u_k \\ -u_k^T & I_2 \end{bmatrix} z^{-1}$, $u_k \in O(2)$ [6].

Lemma 3. Suppose ${}_\gamma P$, ${}_\gamma Q$ are the orthogonal filters defined by (8), then ${}_\gamma P$ satisfies the balanced conditions of order 1 if and only if

$w_0 = r_{-\frac{\pi}{4}}$, or $w_0 = -r_{\frac{3\pi}{4}} D_0$,

where $D_0 = \begin{bmatrix} 1 & 0 \\ 0 & -1 \end{bmatrix}$, $r_\theta = \begin{bmatrix} \alpha_\theta \cos\theta & \sin\theta \\ -\alpha_\theta \sin\theta & \cos\theta \end{bmatrix}$, $\alpha_\theta = \pm 1$.

Definition 2. For a real $r \times 1$ vector function $F = (f_1, \cdots, f_r)^T \in L^2(R)$ supported in $[0, N]$, define the energy moments of F in the time domain by

$$I_F^\beta(y) := \int_{-\infty}^{+\infty} x^\beta F(x) F^T(x - y) dx, \beta \in Z_+.$$

Definition 3. For a real $r \times 1$ vector function $F = (f_1, \cdots, f_r)^T \in L^2(R)$ supported in $[0, N]$, if F is in Sobolev space $W^s(R)$ for some $s \ge 0$, define for β, $0 \le \beta \le 2s$, the energy moments of F in the frequency domain by

$$D_F^\beta(\xi) := \frac{1}{2\pi}\int_{-\infty}^{+\infty} \omega^\beta \hat{F}(\omega) \hat{F}^*(\omega) e^{i\omega\xi} d\omega.$$

Definition 4. For a window function f (with some smoothness and decay at infinity), the center in the time domain $\bar{t}$ and the time-duration Δ_f of f are defined by

$$\bar{t} := \int_{-\infty}^{+\infty} t\left|f(t)\right|^2 dt \Big/ E, \quad \Delta_f^2 := \int_{-\infty}^{+\infty} (t - \bar{t})^2 \left|f(t)\right|^2 dt \Big/ E,$$

where $E := \int_{-\infty}^{+\infty} \left|f(t)\right|^2 dt$. If the Fourier transform $\hat{f}$ of f satisfies $\omega \hat{f}(\omega) \in L^2(R)$, then the center in the frequency domain $\bar{\omega}$ and the frequency-bandwidth $\Delta_{\hat{f}}$ of f are defined by

$$\bar{\omega} := \int_{-\infty}^{+\infty} \omega\left|\hat{f}(\omega)\right|^2 d\omega \Big/ E', \quad \Delta_{\hat{f}}^2 := \int_{-\infty}^{+\infty} (\omega - \bar{\omega})^2 \left|\hat{f}(\omega)\right|^2 d\omega \Big/ E',$$

where $E' := \int_{-\infty}^{+\infty} \left|\hat{f}(\omega)\right|^2 d\omega$.

The product of time-duration and frequency-bandwidth $\Delta_f \Delta_{\hat{f}}$ is called the resolution cell. As the resolution of time and frequency can not be infinitely improved together, in order to get good property of time and frequency, it will have to make $\Delta_f \Delta_{\hat{f}}$ minimized within the scope of which the Heisenberg uncertainty principle confined.

If every component of $\Phi = (\phi_1, \cdots, \phi_r)^T$ and $\Psi = (\psi_1, \cdots, \psi_r)^T$ is normalized, i.e., $\|\phi_j\|_2 = 1$ and $\|\psi_j\|_2 = 1$, then the frequency-bandwidth $\Delta_{\hat{\phi}_j}$ and $\Delta_{\hat{\psi}_j}$ are given by

$$\Delta_{\hat{\phi}_j}^2 = \frac{1}{2\pi}\int_{-\infty}^{+\infty} \omega^2 \left|\hat{\phi}_j(\omega)\right|^2 d\omega, \Delta_{\hat{\psi}_j}^2 = \frac{1}{2\pi}\int_{-\infty}^{+\infty} \omega^2 \left|\hat{\psi}_j(\omega)\right|^2 d\omega \quad (9)$$

Definition 4. The sum of resolution cells $\Delta_{\phi_j}\Delta_{\hat{\phi}_j}$ and $\Delta_{\psi_j}\Delta_{\hat{\psi}_j}$ is called the areas of time-frequency window(also called the window area)

$$S := \sum_{j=1}^r \Delta_{\phi_j}\Delta_{\hat{\phi}_j} + \Delta_{\psi_j}\Delta_{\hat{\psi}_j} \quad (10)$$

To construct multiwavelets with good time-frequency properties means to find scaling functions and multiwavelets that are less in window area S.

III. MAIN ALGORITHM AND RESULT

This paper aims to construct the multiwavelets with good properties of arbitrary order vanishing moment, time-frequency property and regularity through synthetic method of the genetic algorithm and parameterization.

A. The algorithm for computing time-frequency window area

It is not difficult to conclude that the frequency-bandwidth of scaling function and multiwavelet function with high order ($m > 2$)of Jiang's[4] cannot be obtained, which will furthermore influent the calculation of window area under the high order condition. The 2-order energy moments vector in the frequency domain of scaling function Φ and multiwavelet Ψ calculated with the method of Jiang's[4] is the crucial factor in working out the frequency-bandwidth. While the 2-order energy moments vector in the frequency domain is the right $1/4$ eigenvalue of the representation matrix T_P which satisfier specific condition. The order of eigenvalue of representation matrix T_P with its $1/2$ integer power is related with that of the vanishing moment m .If $m<2$, there is no eigenvalue $1/4$ for T_P . If $m>2$, $1/4$ may not be the single eigenvalue of T_P , which means the eigenvalue vector cannot be uniquely destined.

After deep investigating into the relationship between the properties of energy moments in the time and frequency domain of scaling function, the window area of the scaling function and the multiwavelet function that have vanishing moments of arbitrary order can be obtained by using the algorithm of calculating the time-frequency window area, which can choose the method of calculating the frequency-bandwidth according to the count of 1/4 eigenvalue of representation matrix T_P of the multiwavelet. Finally, the window area of the multiwavelet is worked out. If the 1/4 eigenvalue of representation matrix T_P is simple, then the frequency-bandwidth $\Delta_{\hat{\phi}_j}$ and $\Delta_{\hat{\psi}_j}$ for the components of scaling functions and multiwavelet functions can be worked out using the 2-order energy moments vector in the frequency domain. Otherwise, $\Delta_{\hat{\phi}_j}$ and $\Delta_{\hat{\psi}_j}$ can be obtained by the formula of (3), (4) and compound Simpson. The window area S of scaling function and multiwavelets is finally worked out by using formula (10).

The new algorithm for the area of time-frequency window is as follows:

Step 1: Find the time-duration Δ_{ϕ_j} and Δ_{ψ_j} of the components of scaling functions and multiwavelet functions with 1 or 2-order energy moments vector in the time domain.

Step 2: Work out the eigenvalues of the representation matrix T_P

a) If $1/4$ is a single eigenvalue, then find the frequency-bandwidths $\Delta_{\hat{\phi}_j}$ and $\Delta_{\hat{\psi}_j}$ of scaling functions and multiwavelet functions with the 2-order energy moments vector in the frequency domain, else

b) Use the cascade formula (3), (4) and compound Simpson formula to find the frequency-bandwidths (9).

Step 3: Compute the window area S of the scaling functions and multiwavelet functions with formula (10).

The main body of cascade formula (3) is $\hat{\Upsilon}_n(\omega)$. If ω multiplicate n_1 times ($n_1=8$), where $\omega\in[-2^{n_1}\pi,2^{n_1}\pi]$, and ω is equally separated to $2^{n_1+n_2+1}$ parts with the step length of $\frac{\pi}{2^{n_2}}$, then the time complexity of the cascade formula (3) is $O((n_1+1)2^{n_1+n_2+1})$. During the calculation of compound Simpson formula, the lower limit of integration $a=-2^{n_1}\pi$, the upper limit $b=2^{n_1}\pi$, with the step length $h=\pi/2^{n_2}$. thus $n=2^{n_1+n_2}$. In order to control the error within 10^{-5}, let $n_2=6$.

In fact, $\phi_j(t)$ and $\psi_j(t)$ are aperiodic continuous functions in their time-duration $[0,N]$, and the Fourier transform $\hat{\phi}_j(\omega)$ and $\hat{\psi}_j(\omega)$ of them are aperiodic continuous functions in their frequency-bandwidths $(-\infty,+\infty)$. As the attenuation of the window function W is a compulsory condition, which means if $|\omega|\to\infty$, then $|\hat{W}(\omega)|\to 0$, and the attenuation of $\hat{W}(\omega)$ gets faster with smoother window function W . It is feasible letting the lower limit and upper limit of integration in compound Simpson formula to be $-2^{n_1}\pi$ and $2^{n_1}\pi$ respectively.

B. New algorithm of designing balanced symmetric orthogonal multifilter banks

This paper aims to construct the balanced symmetric orthogonal multifilter banks with arbitrary order vanishing moments through synthetic method of parameterization and solving the nonlinear equations of vanishing moment conditions.

Step 1: Construct the parameterized representation of multifilter banks P and Q which satisfy the conditions of orthogonality and balanced of order 1. P and Q can be expressed as (6):

Step 2: Find the parameter that has maximum Sobolev regularity through the method of genetic algorithm.

Step 3: Find the parameter that makes the minimum window area through the method of genetic algorithm.

Step 4: Derive the conditions of vanishing moment of each order out according to Proposition 1.

Step 5: Solve the nonlinear equations of vanishing moment conditions. Thus determine the parameter value of P and Q . Then, compute the corresponding window area out.

Step 6: If the solution of vanishing moment condition is not unique, then

Select the parameter that makes the maximum Sobolev regularity.

Select the parameter that makes the minimum window area.

Select the parameter which makes good perform both in regularity and time-frequency properties.

Step 7: Verify that whether the representation matrix T_P of lowpass filter corresponding to the selecting parameters can satisfy the condition E [9] .

Although these multifilter banks only produce scaling functions and multiwavelet functions with approximate symmetry, the parameterized form of ${}_{\gamma}P$ can not only satisfy the condition of 1-order balance, but also has γ free parameters, which is suitable to use in constructing the balanced symmetric orthogonal multifilter banks with vanishing moment of high order and smoothness.

During the 4th step of the algorithm, the vanishing moment condition of each order with parameters are obtained. Thus the problem turns to the solving of nonlinear equations. In this paper, the classical Newton algorithm and secant algorithm are used, during which the error $|\varepsilon| < 10^{-14}$.

C. Construction result

The scaling function $\Phi = (\phi_1, \phi_2)$ corresponding to the balanced symmetric orthogonal multifilter banks constructed in this paper has the properties such as:

a) Φ is balanced and orthogonal;

b) The matrix lowpass filter of ϕ_1 and ϕ_2 are symmetric;

c) The length difference of matrix lowpass filter of ϕ_1 and ϕ_2 is 4.

Table I shows the properties of the balanced symmetric orthogonal multifilter banks constructed in this paper when $\gamma = 2,3,4$. When the supported in [0, $2\times\gamma+1$] and the vanishing moment is N-order, Oγ _VN and Sγ _VN represent those multifilter banks of optimum time-frequency resolution and optimum regularity, and OS γ _VN represent those of good time-frequency resolution and regularity properties concerned together. Here, Oγ _VN and OSγ _VN are provided by this paper for the first time, and S2_V2, S3_V3, S4_V3 are the same in properties to Jiang's [6].

TABLE I. CONTRASTING OF PROPERTIES BETWEEN VARIOUS MULTIWAVELETS

Multi-wavelet	Support	Regularity	Vanishing moment	Window area
GHM	3	1.4999	2	8.1492
J_EX2	3	1.7470	2	9.2793
J_EX4	5	1.7018	2	8.9565
O2_V2	5	1.0000	2	5.7427
S2_V2	5	1.5379	2	5.7706
O3_V2	7	1.5842	2	7.1738
S3_V2	7	1.9984	2	7.6951
OS3_V2	7	1.9911	2	7.5803
O3_V3	7	1.9983	3	7.6961
S3_V3	7	2.0953	3	9.3950
OS3_V3	7	1.9883	3	7.7421
O4_V2	9	1.0000	2	5.6579
S4_V2	9	1.9967	2	6.4761
OS4_V2	9	1.9082	2	5.7589
O4_V3	9	1.5890	3	5.7281
S4_V3	9	2.3583	3	12.1789
OS4_V3	9	2.0460	3	7.3696

We representatively list the coefficients of OS3_V3 as follows, which is good in regularity and time-frequency resolution with 3-order vanishing moment.

$a_0 =$ -0.00722419185700 , $a_1 =$ 0.02517755242000 ,

$a_2 =$ -0.01657868919500 , $a_3 =$ -0.05777958621500 ,

$a_4 =$ 0.06500377807200 , $a_5 =$ 0.49140113677500 ,

$b_0 =$ 0.00045619860800 , $b_1 =$ -0.00158993069200 ,

$b_2 =$ 0.00131515341700 , $b_3 =$ 0.00458353609100 ,

$b_4 =$ 0.01561574451800 , $b_5 =$ -0.09976122681300 ,

$b_6 =$ 0.10003600408800 , $b_7 =$ 0.47934452078400 ,

$c_0 =$ -0.00459388502300 , $c_1 =$ 0.01601048023800 ,

$c_2 =$ -0.01749108641000 , $c_3 =$ -0.06095944759900 ,

$c_4 =$ 0.25325770936800 , $c_5 =$ -0.42609987213500 ,

$d_0 =$ -0.00045619860800 , $d_1 =$ 0.00158993069200 ,

$d_2 =$ -0.00131515341700 , $d_3 =$ -0.00458353609100 ,

$d_4 =$ -0.04968552012300 , $d_5 =$ 0.21850026062700 ,

$d_6 =$ -0.08821792720800 , $d_7 =$ -0.43815648812600 ,

Contrast with the OPTFR multiwavelets of Jiang's [4], our multifilter banks in this paper have the advantages as follows

a) The multifilter banks with optimum time-frequency resolution constructed in this paper have the vanishing moment of 3-order, comparing with the 2-order of Jiang's.

b) J_EX2 and J_EX4 are the multiwavelets listed in Jiang's [4] as example 2 and 4. These orthogonal OPTFR multiwavelets are not balanced. Although we can further make them balanced by reversing the original multiwavelets for $\pi/4$ angle, the symmetry of the balanced multiwavelets and the multifilter banks would be lost, which are not optimum in its time-frequency property any longer. The multifilter banks constructed in this paper are not only balanced, but also have the balanced optimum time-frequency resolution and the symmetry properties as concerned in formula (6).

c) The window area of multifilter banks we constructed is smaller than those of Jiang's [4]. For example, the window area of O2_V2 is 3.2 smaller than J_EX4, with their support being both 5. Although the support of O3_V2, OS3_V2, O3_V3, OS3_V3, O4_V2, OS4_V2, O4_V3 and OS4_V3 are longer than Jiang's, the window areas of them are all smaller by contraries.

IV. APPLICATION IN IMAGE PROCESSING

In order to test the performances of the balanced symmetric orthogonal OPTFR multiwavelets constructed in our research, we use the standard 512×512 grey image named Lena, Baboon and Barbara to do the simulating experiment, in which Barbara and Baboon are texture images, and Lena is the typical smooth image. As i)wavelets CDF9-7, DB4 and multiwavelet SA4 performing well in image processing, ii)multiwavelet GHM being similar in form of multifilter bank with ours, iii) J_EX2 and J_EX4 being the best two OPTFR multiwavelets of Jiang's[4], we choose these wavelets/multiwavelets to do our experiment.

A. Application in image denoising

During the experiment, we first produced three kind of noise image of different intensity ($\sigma = 10,20,30$). Then, with each kind of noise image decomposed to three degree, the denoising is pursued with Donoho's SureShrink [9] threshold value program. Finally, the denoising images are reconstructed with multiwavelet inverse transformation. Table II shows the peak signal to noise ratio (PSNR) of noising image and reconstructed denoising image. As shown in fig.1, the summery of denoising appreciation index (adding three PSNRs in the same row of Table II) to every multiwavelet for Barbara, Baboon and Lena are listed. In fig.2, a) is the original image of Lena, b), c) and d) are the denoising image processed by OS3_V3, J_EX2 and SA4 seperately, based on the noising image of Lena with $\sigma = 20$ (not showed here). Likewise, in fig.3, a) is the original image of Barbara, b),c) and d) are the denoising image processed by OS3_V3, J_EX2 and SA4 seperately.

The experiment results show that:

a) The multifilter banks we have constructed are obviously better than multiwavelet GHM in image denoising. Moreover, the advantages become bigger with more noise. For texture image Barbara and Baboon, the value of PSNR is higher for 0.71 to 1.61dB; for image Lena, it is also higher for 1.04 to 3.14dB. Especially for multiwavelet O2_V2, it is lower in regularity for 0.5 and smaller in time-frequency window area for 2.4 contrasting with GHM when their vanishing moment is equivalent.

TABLE II. PSNR OF WAVELETS/MULTIWAVELETS UNDER DIFFERENT NOISING VARIANCE

NO.	**Wavelet/ multiwavelet**	**Barbara**			**Baboon**			**Lena**		
		$\sigma=10$	$\sigma=20$	$\sigma=30$	$\sigma=10$	$\sigma=20$	$\sigma=30$	$\sigma=10$	$\sigma=20$	$\sigma=30$
		28.1496	22.2005	18.8001	28.1474	22.1198	18.6556	28.1167	22.1389	18.7202
1	GHM	30.6647	26.3682	23.9871	28.3819	25.0009	22.8704	32.5039	27.9962	25.3866
2	J_EX2	30.5197	26.9376	25.0078	27.9729	24.8689	23.2836	33.2071	30.1380	28.3591
3	J_EX4	29.1941	25.5981	23.8247	26.8960	23.9753	22.4742	31.8879	28.6367	26.8396
4	SA4	31.2018	27.5280	25.5348	28.1598	25.1245	23.4536	33.4509	30.3375	28.5072
5	DB4	30.7848	27.0461	25.0840	28.0645	24.8914	23.3249	33.2711	30.1076	28.2982
6	CDF9-7	30.7179	27.0756	25.1927	28.0427	24.9556	23.3010	33.4065	30.2667	28.4657
7	O2_V2	30.6660	26.9326	25.0046	27.9327	24.9578	23.2667	33.2412	30.1116	28.2402
8	S2_V2	30.6605	26.9206	25.0069	27.9469	24.9486	23.2635	33.2448	30.1110	28.2377
9	O3_V2	31.0349	27.2572	25.2795	28.1598	24.9970	23.3488	33.4039	30.2302	28.4100
10	S3_V2	**31.3730**	27.5580	25.5221	28.2497	25.0891	23.3940	33.5263	30.3600	28.5241
11	OS3_V2	31.3384	27.5298	25.5045	28.2603	25.0936	23.3923	33.5374	30.3574	28.5213
12	O3_V3	31.3638	27.5615	25.5203	28.2466	25.0893	23.3938	33.5266	30.3601	**28.5243**
13	S3_V3	31.3405	**27.6143**	**25.5979**	**28.3081**	**25.0974**	23.3776	33.5227	30.3168	28.4890
14	OS3_V3	31.3607	27.5560	25.5357	28.2769	25.0810	23.3843	**33.5485**	**30.3669**	28.5214
15	O4_V2	30.7447	27.0463	25.0754	28.0922	24.9631	23.2851	33.2771	30.1425	28.3025
16	S4_V2	31.1218	27.2738	25.2918	28.1366	25.0389	23.3521	33.4648	30.3021	28.4240
17	OS4_V2	30.8504	27.0896	25.1459	28.0207	24.9708	23.3328	33.3107	30.175	28.3244
18	O4_V3	30.6640	26.9901	25.0428	27.9602	24.9712	23.3036	33.2850	30.1262	28.2907
19	S4_V3	30.9655	27.3312	25.4186	27.9920	24.9662	23.3051	33.1317	30.0562	28.2978
20	OS4_V3	31.2181	27.4192	25.5081	28.1779	25.0504	**23.4058**	33.4454	30.2709	28.4707

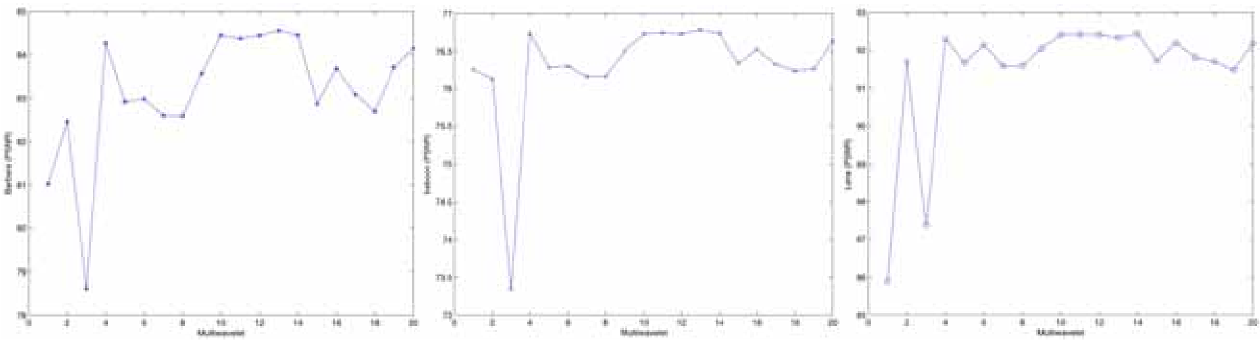

a) Barbara b) Baboon c) Lena

Figure 1. Denoising performance of different Wavelet/Multiwavelet

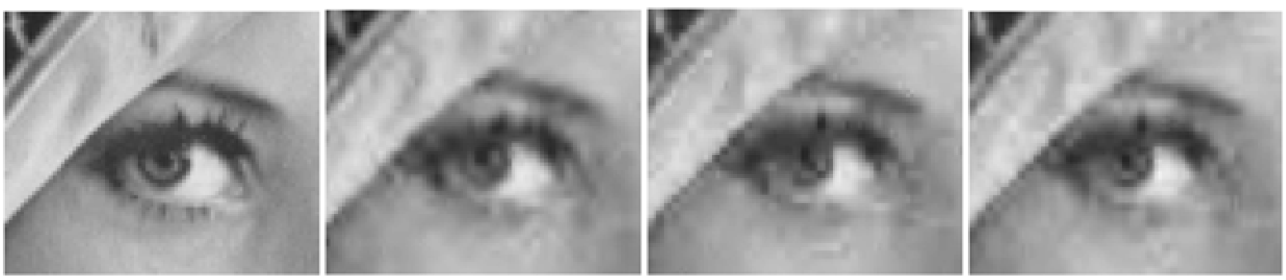

a)the original image of Lena b) OS3_V3 c) J_EX2 d) SA4

Figure 2. Denoising performance of different Wavelet/Multiwavelet with Lena ($\sigma = 20$)

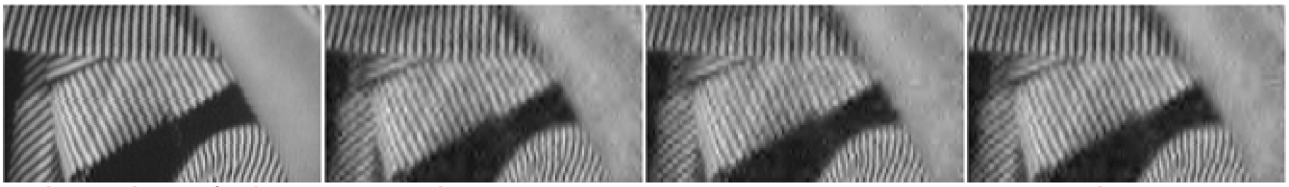

a)the original image of Barbara b) OS3_V3 c) J_EX2 d) SA4

Figure 3. Denoising performance of different Wavelet/Multiwavelet with Barbara ($\sigma = 20$)

Further more, its performance with Lena and Barbara are greatly better than GHM.

b) Contrast with multiwavelet J_EX4(NO.3), multiwavelet O2_V2(NO.7) has the same support, but lower in regularity for 0.7 and smaller in time-frequency window area for 3.2, which makes good greatly for its performance in image denoising. In fig. 1, we can see that O2_V2 perform better in denoising for all the three images than J_EX2 (NO.2), which was the best multiwavelet of Jiang's.

c) As shown in fig. 1, from multiwavelet SA4(NO.4) to wavelet CDF9-7(NO.6) and DB4(NO.5), the denoising performance decrease in turn, and SA4 is the best one at present. However, the synthetic performances of our multiwavelets(NO10. TO NO.14) in image denoising are better than SA4.

In summery, the multifilter banks constructed in this paper have good performances in both texture image and smooth image. Especially for S3_V2, OS3_V2, O3_V3, S3_V3 and OS3_V3, their performances in image denoising are better than not only the best multiwavelet SA4, but also the best wavelet CDF9-7 at present.

TABLE III. PSNR OF WAVELETS/MULTIWAVELETS IN COMPRESSING WITH DIFFERENT COMPRESSING RATIO

NO.	**Wavelet/ multiwavelet**	**Barbara**			**Baboon**			**Lena**		
		16:1	32:1	64:1	16:1	32:1	64:1	16:1	32:1	64:1
1	GHM	28.1833	25.1393	23.3500	24.6406	22.7511	21.4624	34.5513	31.1196	28.1739
2	J_EX2	29.7339	26.1370	23.6241	25.3085	23.0975	21.6889	35.6398	32.0850	28.6669
3	J_EX4	26.5333	24.0995	22.2643	24.0833	22.1177	21.0473	32.4086	28.8778	25.8550
4	SA4	29.5402	26.0751	23.6423	25.3112	23.0124	21.6230	35.6983	31.9372	28.4684
5	DB4	29.9789	26.2356	23.6681	25.3216	23.0708	21.6884	35.6657	31.9305	28.3906
6	CDF9-7	30.3255	26.4018	23.7980	25.5048	23.1999	21.7113	36.3287	32.7832	29.2587
7	O2_V2	29.7733	26.1491	23.5683	25.2666	**23.0666**	**21.6941**	**35.5921**	31.8970	28.4569
8	S2_V2	29.7684	26.1465	23.5672	25.2639	23.0629	21.6931	35.5884	31.8877	28.4530
9	O3_V2	29.3660	26.1106	23.5552	25.2353	23.0083	21.6464	35.2839	31.6400	28.3022
10	S3_V2	29.8516	26.4345	23.7064	25.3399	23.0522	21.6706	35.5838	31.8972	28.5129
11	OS3_V2	29.7959	26.3964	23.6811	25.3300	23.0404	21.6701	35.5467	31.8634	28.4922
12	O3_V3	29.8511	26.4346	23.7065	25.3400	23.0525	21.6706	35.5837	31.8972	28.5138
13	S3_V3	29.8952	**26.5441**	**23.7693**	25.3255	23.0454	21.6464	35.5271	31.7922	28.4498
14	OS3_V3	29.8723	26.4444	23.7158	**25.3431**	23.0616	21.6750	35.5883	**31.9071**	28.5120
15	O4_V2	29.9025	26.2353	23.6407	25.2453	23.0454	21.6685	35.4364	31.7293	28.4307
16	S4_V2	29.7660	26.2629	23.6102	25.2441	23.0298	21.6611	35.5408	31.8207	28.4149
17	OS4_V2	**30.0384**	26.3106	23.6948	25.2863	23.0537	21.6729	35.5757	31.8335	**28.5172**
18	O4_V3	29.7399	26.1538	23.5989	25.2154	23.0249	21.6555	35.3598	31.6691	28.3744
19	S4_V3	29.8048	26.2381	23.6644	25.2151	22.9445	21.6063	34.7106	31.3981	28.2485
20	OS4_V3	29.8185	26.4303	23.7256	25.3054	23.0149	21.6471	35.4291	31.7070	28.4855

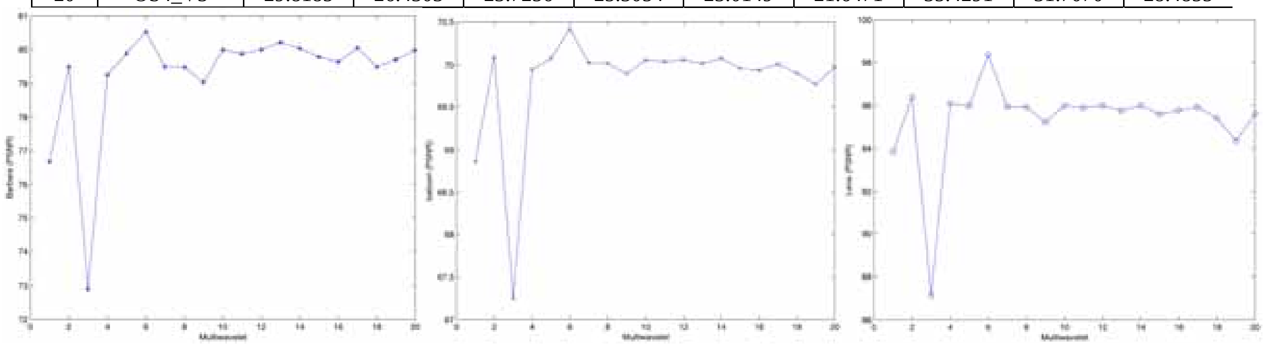

a) Barbara b) Baboon c) Lena

Figure 4. Compressing performance of different Wavelet/Multiwavelet

B. *Application in image compression*

During the experiment, the multiwavelet is decomposed to 5 degree first. Then, job of quantification and compression are done by the improved SPIHT algorithm [12]. Finally, decoding for SPIHT bit current and image reconstructing through multiwavelet inverse transformation are performed. As the aim of our experiment is to contrast with the different performances of various multiwavelets/wavelets, the process of arithmetic coding for bit current which is coded by SPIHT is neglected. The contrasting experiment based on SPIHT bit current can well demonstrate the difference performances of the multifilter/filter banks. Table III shows the values of PSNR for the multiwavelets/ wavelets dealing with Barbara, Baboon and Lena with the compression rate of 16:1, 32:1 and 64:1 .

From the experiment we found that:

a) The performances of the multifilter banks we constructed in image compression are obviously better than that of GHM. As for image Barbara, Baboon and Lena, the value of PSNR of our result is higher than that of GHM for 0.42 to 1.86dB, 0.23 to 0.70dB and 0.34 to 1.04dB separately.

b) From fig. 4 we know, as for the three images we chose, most of our multifilter banks performed better than J_EX4 in image compression. As J_EX2 being the OPTFR multiwavelet of Jiang's[4] with shortest supported in [0,3], most of our multifilter banks performed better than J_EX2 in compression with Barbara, and approximate J_EX2 with Baboon.

c) As shown in a) and b) of fig. 4, the best performances in compressing with texture image Barbara and Baboon are made by wavelet CDF9-7, wavelet DB4 and multiwavelet SA4. However, most of our multiwavelets are synthetically better performed than the best multiwavelet SA4, and better than or approximate that of wavelet DB4.

Image compression experiments show that, the performances of most of our multiwavelets are better than that of SA4 and approximate wavelet DB4.

It is not difficult to see that, the performances of OS3_V2, S3_V2, O3_V3, S3_V3, OS3_V3 in image compression are better than that of the others especially when dealing with texture images.

V. CONCLUSION

In this paper, construction method is improved to obtain the multifilter banks that have good properties and better performances in image processing. By introduce the time-frequency property to the construction of balanced symmetric orthogonal multifilter banks, we first obtained the optimum time-frequency resolution multifilter banks which have arbitrary vanishing moment. With the properties of vanishing moment, regularity, time-frequency resolution synthetically concerned, we first constructed the multifilter banks which have good performances both in regularity and time-frequency resolution. Furthermore, the smoothest balanced symmetric orthogonal multifilter bank is obtained. Application experiments in image processing show that, the performances of most of our multifilter banks in image denoising are better than that of multiwavelet SA4 and wavelet CDF9-7. As for image compression, their performances are better than that of SA4 and approximate wavelet DB4.

REFERENCES

[1] Haddad RA, Akansu AN, Benyassine A. Time-frequency localization in transforms, subbands, and wavelets: A critical review. Optical Engineering, 1993, 32(6): 1411-1429.
[2] Morris M, Akunuri V, Xie M. More results on orthogonal wavelets with optimum time-frequency resolution. In: Proc S.P.I.E. 2491, 1995, 52-62.
[3] Jiang Q. On the Design of Multifilter Banks and Orthonormal Multiwavelet Bases, IEEE Trans. Signal processing, 1998, 46: 3292-3303.
[4] Jiang Q. Orthogonal multiwavelets with optimum time-frequency resolution. IEEE. Trans. Signal Processing, 1998, 46(4): 830-844.
[5] Xia T, Jiang Q. Optimal multifilter banks: Design, related symmetric extension transform and application to image compression. IEEE Trans. Signal Processing, 1999, 47, 1878-1889.
[6] Jiang Q. Parametrizations of symmetric orthogonal multifilter banks with different filter lengths, Linear Algebra and its Applications, 2000, 311, 79-96.
[7] Cohen A, Daubechies I, Plonka G. Regularity of refinable function vectors. Fourier Anal. Appl. 1997, 3. 295-323.
[8] Chen D, Construction of Smooth Refinable Function Vectors by Cascade Algorithms. SIAM J. Math. Anal, 2002 40(4): 1354-1368.
[9] Shen Z. Refinable function vectors. SIAM J. Math. Anal, 1998, 29(1): 235-250.
[10] Plonka G. Approximation order provided by refinable function vectors. Constr. Approx, 1997, 13, 221-224.
[11] Jiang Q. On the regularity of matrix refinable functions. Soc. Indus. Appl. Math. J. Math. Anal, 1998, 29, 1157-1176.
[12] Martin MB, Bell AE. New image compression Techniques using multiwavelets and multiwavelet packets, IEEE Trans. Image Compression, 2001, 4(10): 500-510.
[13] Goodman T.N., Lee S.L. and Tang W.S., Wavelets in wandering subspaces, Trans. Amer. Math. Soc., 1993, 338:639-654.
[14] Donoho DL, Johnstone IM. Adapting to unknown smoothness via wavelet shrinkage. Journal of the American Statistical Association, 1995, 90,1200-1224.
[15] Gao Xieping, Zhou Siwang. A study of orthogonal, balanced and symmetric multi-wavelets on the interval.Science in China. Series f, Information Sciences,2005,48(5):761-781.
[16] Gao Xieping, Cao Chunhong. Minimum-energy wavelet frame on the interval.Science in China Series F-information. Science, 2008, 51(10): 1547-1562.

Zeng Zhaohui was born in Hunan, China, on Aug. 26, 1977, received her B.S. degree and M.S. degree in computer software from Xiangtan University, Xiangtan, China, in 2000 and 2007 respectively.

She is a lecture in Xiangtan University. Her current research interests are in wavelet/multiwavelet and image processing.